

Thermochromism in polydiacetylene-metal oxide nanocomposites

Anitha Patlolla,^a James Zunino, III,^b Anatoly I. Frenkel^c and Zafar Iqbal^{*a}

Received 26th November 2011, Accepted 7th February 2012

DOI: 10.1039/c2jm16175c

Irreversible and reversible chromatic transitions during heating and cooling cycles were investigated in polydiacetylene poly-PCDA (poly-10,12-pentacosadiynoic acid) composites with nanocrystalline zinc oxide (ZnO), titanium oxide (TiO₂), zirconium oxide (ZrO₂) and ZnO and ZrO₂ alloys. In contrast to pure poly-PCDA, poly-PCDA composites with nanocrystalline ZnO displayed rapid reversibility on thermal cycling, whereas the corresponding composites with nanocrystalline TiO₂ and ZrO₂ were irreversible, and poly-PCDA composites with thermally prepared ZnO and ZrO₂ alloys displayed slower reversibility. The mechanism of reversible and irreversible thermochromism in these materials was explored using Raman spectroscopy, Fourier transform infrared spectroscopy (FTIR), differential scanning calorimetry (DSC) and X-ray absorption fine structure (XAFS) spectroscopy. In pure poly-PCDA, heating leads to an irreversible strain on the polymer backbone to form a red phase, which is not released on cooling. In the presence of ZnO evidence is provided for chelation involving the side chain head groups which can release strain on cooling to rapidly form the blue phase. Chemical interaction coupled with reversible behavior was however observed only when the composites were prepared with ZnO having an average crystallite size of 300 nm and below with a fraction of an amorphous grain boundary phase. Poly-PCDA composites with ZnO/ZrO₂ alloys showing slower thermochromic reversibility can be used both as temperature and elapsed time-temperature sensors.

Introduction

Solid state topotactic photo-polymerization of diacetylenes by exposure to UV radiation and subsequent thermochromism in closely packed and uniformly ordered thin films of various polydiacetylenes (PDA's) are well known.¹ Liquid state polymerization studies of the monomers have also been reported.^{2–6} PDA's have a one dimensional conjugated backbone with a strong π to π^* absorption band in the red spectral region of the optical spectrum giving rise to an intense blue color. The blue phase undergoes a thermochromic transition observed in many PDA's to a red phase on heating. The blue to red chromatic transition is either irreversible or reversible under heating and cooling cycles depending on the chemical structure and interactions on the side chains. The chromatic transition can also be initiated by mechanical stress, change of pH or ligand-receptor interactions.^{7–17} The blue to red thermochromic transition in different PDA's has also been explained in terms of bond exchange in the conjugated backbone,¹⁸ changes in the molecular conformation,¹⁹ reorganization of the side

groups,^{20,21} and change of the alkyl side chains to more ordered states.

In the blue phase, heat-induced strain on the polymer backbone *via* side chain head group interactions leads to the formation of the red phase.²² The red phase can rapidly reverse back to the blue phase on cooling when: (a) strong head group aromatic interactions,²³ (b) ionic interactions,²⁴ (c) covalent interactions,^{25,26} (d) enhanced hydrogen bonding at the head groups,^{27–29} and (e) multiple hydrogen bonding,^{30–35} are present in the PDA structures. Reversible chromatic transitions also occur in photopolymerized phosphatidylcholine-PDA vesicles,³⁶ organic-inorganic hybrids of PDA's with sodium hydroxide,³⁷ lithium compounds,³⁸ mesoporous silica and layered double hydroxide.³⁹ The red phase is irreversible when the head group interactions remain firmly in place and cannot be reversed on cooling.

The blue to red thermochromic transitions in PDA's are therefore broadly of two types: irreversible and reversible. Here, a facile method to induce both reversibility and partial irreversibility of the thermochromic transition in a material with an irreversible transition is presented. It was found that the polydiacetylene, 10,12-pentacosadiynoic acid (poly-PCDA), can form nanocomposites with nanocrystalline inorganic oxides: zinc oxide (ZnO),⁴⁰ titanium oxide (TiO₂),^{41,42} zirconium oxide (ZrO₂), and ZnO and ZrO₂ alloys, to form PDA nanocomposites with thermochromic transitions ranging from irreversible to partially and fully reversible. The addition of nanocrystalline ZnO to poly-PCDA rapidly reverses the red phase on cooling

^aDepartment of Chemistry and Environmental Science, New Jersey Institute of Technology, Newark, NJ, 07102, USA. E-mail: iqbal@adm.njit.edu

^bU.S. Army Armament Research, Development and Engineering Center, RDAR-MEE-M, Picatinny Arsenal, NJ, 07806, USA

^cDepartment of Physics, Yeshiva University, 245 Lexington Avenue, New York, NY, 10016, USA

and at the same time substantially increases the chromatic transition temperature. An understanding of the influence of the oxides on the molecular structure of poly-PCDA was achieved by temperature-dependent Raman spectroscopy, Fourier-transform infrared (FTIR) spectroscopy, colorimetric measurements, differential scanning calorimetry (DSC), X-ray powder diffraction (XRPD) and X-ray absorption fine structure (XAFS) spectroscopy. The effect of ZnO crystallite size and ZnO/ZrO₂ alloys on modifying the thermochromic transition was studied and use of the mixed oxides as elapsed time-temperature indicators was briefly evaluated.

Experimental

Materials

PCDA was purchased from GFS Chemicals and nanocrystalline inorganic oxides ZnO and ZrO₂, and micron-sized, puriss ZnO were purchased from Sigma-Aldrich. Nanocrystalline TiO₂ was purchased from Degussa. Passivated nanocrystalline ZnO with size in the 2.1 nm range was provided by D.S. Lee and K.W. Lem, Konkuk National University, Seoul, South Korea. Samples of ZnO alloyed with ZrO₂ were prepared as described below. Analytical grade solvents, such as chloroform and acetone from Sigma-Aldrich, were used without further purification.

Synthesis of poly-PCDA-metal oxide nanocomposites

Poly-PCDA-ZnO suspensions were prepared by suspending 0.02 gm of ZnO in 2 mM solution of PCDA monomer in chloroform. The suspension was sonicated in a water bath at room temperature for about 30 min. A similar procedure was used to make a suspension with TiO₂ and ZrO₂, and drops of the suspensions were deposited on a glass slide followed by solvent evaporation at room temperature to form thin films, which were polymerized to the blue phase of poly-PCDA composites by irradiating with a 254 nm wavelength UV source. Powders of the blue phase composites were obtained by scraping from the glass slide and grinding into a fine powder. Red phase composite powders and films were similarly produced after heating the blue phase to above the thermochromic transition temperature.

Synthesis of poly-PCDA-ZnO/ZrO₂ nanocomposites

Nanocrystalline (nc) powders of ZnO and ZrO₂ were obtained from Sigma-Aldrich. A mixture of nominal composition Zn_{0.2}Zr_{0.8}O_y was finely ground using a mortar and pestle, transferred to a ceramic boat and heated in a furnace in air at 1100 °C for about 7 h. The heat-treated ZnO/ZrO₂ mixture was then ground into a fine powder and mixed with PCDA monomer to prepare composites of poly-PCDA by a procedure similar to that described above for preparing composites with the pure metal oxides.

Measurement and techniques

Raman spectroscopy. Raman spectra at room temperature were obtained primarily using a Mesophotonics Raman spectrometer with 785 nm laser excitation. Temperature-dependent Raman measurements were carried out with an EZRaman LE Raman Analyzer system from Optronics using 785 nm laser excitation

coupled to a Leica optical microscope. The spectrometer was calibrated using silicon wafer and diamond powder standards to a frequency accuracy of ± 1 cm⁻¹. The variable temperature optical stage used is from Linkam Scientific Instruments Ltd. Thick films for the Raman measurements were prepared by mixing suspensions of PCDA with those of ZnO, ZrO₂, TiO₂ or ZnO/ZrO₂ alloys in the ratio of 1 : 1 percent by weight using chloroform as the suspension medium. Films were deposited by drop coating on a silicon wafer substrate and polymerized to the blue phase of poly-PCDA by irradiating with 254 nm uv-radiation. The blue phase films were heated above the chromatic transition temperature to polymerized films of the red phase.

FTIR spectroscopy. The FTIR spectra were obtained using a Perkin Elmer 100-R spectrometer. KBr pellets for FTIR spectroscopy were prepared by mixing PCDA with nanocrystalline ZnO in a 1 : 1 ratio and this mixture was combined with KBr and pressed into pellets in a die. The pellets obtained were thin, transparent and colorless, which on exposure to UV radiation converted to the blue phase of poly-PCDA-ZnO. The blue phase was heated above the chromatic transition temperature to the red phase. The same procedure was used to obtain KBr pellets of poly-PCDA composites with TiO₂ and ZrO₂. Since the red phase rapidly converts back to the blue phase in ZnO composites at room temperature, the spectra were recorded immediately after heating, but the spectra obtained were typically those of a mixture of the red and blue phases.

UV-visible spectroscopy. The UV-visible spectra of poly-PCDA-ZnO composites were obtained at room temperature using an Agilent 8453 UV-visible spectrometer. About 0.02gm ZnO of three different particle sizes were suspended in a 2mM solution of PCDA in chloroform and bath-sonicated. The suspensions obtained were spin-coated on glass slides at the rate of 2000 rpm to obtain highly transparent thin films which were then polymerized by 254 nm UV radiation to the blue phase and converted to the red phase by thermal treatment above the chromatic transition temperature.

Optical densitometry. Chromaticity, which is a quantitative measure of the vividness or dullness of a color (or how close the color is to either the gray or pure hue) was measured directly on thin film and coated samples using an X-Rite 518 optical densitometer.

Differential Scanning Calorimetry (DSC). A Mettler Toledo DSC instrument with a FP90 central processor was used to obtain the DSC data of 10 mg of precursor, polymer and composite samples wrapped in a small disk with aluminium foil using heating/cooling/heating cycles in the temperature range from 0° to 200 °C at a rate of 10 °C min⁻¹.

X-Ray Powder Diffraction (XRPD). The XRPD patterns were obtained at room temperature as films or powders on a silicon wafer substrate with a Philips X'pert diffractometer using Cu-K α radiation at $\lambda = 1.54$ Å, voltage = 45 kV, current = 40 amps.

Particle size measurements. The average particle size distributions were determined using a Beckmann Coulter size

analyzer. The powders were suspended in acetone in a closed container, left standing overnight and the top supernatant was used for size distribution analysis.

X-ray Absorption Fine Structure (XAFS). Powders of poly-PCDA nanocomposites prepared using the methods described above, together with their respective pure nanoscale oxides, were used for the XAFS measurements, which were carried out using the beamlines X18B and X19A at the National Synchrotron Light Source at the Brookhaven National Laboratory, Upton, New York. All data were measured at the Zn K-edge using Si (111) monochromator which was 30% detuned to reduce higher harmonics.

Results and discussion

The nature of the interactions at the molecular level between the oxides and the polydiacetylene head groups in: i) poly-PCDA, ii) poly-PCDA-ZnO nanocomposites, iii) poly-PCDA-ZrO₂ nanocomposites, iv) poly-PCDA-TiO₂ nanocomposites, and v) poly-PCDA-ZnO/ZrO₂ composites, were investigated using Raman, FTIR and UV-visible spectroscopy together with DSC, XRPD and XAFS measurements. The studies discussed below were made on composite samples prepared using pure oxides with particle sizes near and below 300 nm.

Poly-PCDA nanocomposites

The FTIR spectra in Fig. 1 of the blue and red phases of pure poly-PCDA and poly-PCDA nanocomposites show lines at 2965 and 2870 cm⁻¹ due to the asymmetric and symmetric stretching

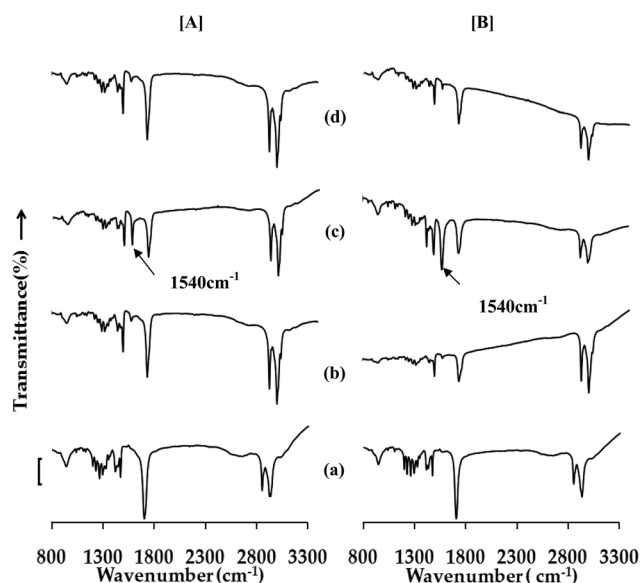


Fig. 1 FTIR spectra at 25 °C of pure poly-PCDA and poly-PCDA nanocomposites with nanocrystalline metal oxides in the blue (panel A) and red (panel B) phases in the 800–3300 cm⁻¹ region. The spectra shown are of: (a) pure poly-PCDA, (b) poly-PCDA composite with TiO₂, (c) poly-PCDA composite with ZnO, and (d) poly-PCDA composite with ZrO₂. The height of the square bracket on the bottom left hand corner corresponds to 20% transmittance. The arrows indicate the line at 1540 cm⁻¹ discussed in the text.

vibrations of the CH₂ groups of the polydiacetylene side chains. The lines at 1465, 1420 and 1697 cm⁻¹ can be assigned to the CH₂ scissoring vibrations and hydrogen-bonded carbonyl C=O stretching vibrations, respectively. A new, relatively strong line appears at 1540 cm⁻¹ in the nanocomposite with ZnO, while the line at 1697 cm⁻¹ decreases in intensity in both the blue and red phases of poly-PCDA-ZnO. The 1540 cm⁻¹ line is also seen as a weak feature in poly-PCDA nanocomposites with TiO₂ and ZrO₂. The FTIR spectra of blue and red poly-PCDA-ZnO in the 700–1900 cm⁻¹ range showing more clearly the increase in intensity of the 1540 cm⁻¹ line and the decrease in intensity of the line at 1697 cm⁻¹ (relative to that near 720 cm⁻¹) is shown in Fig. 2. The 1540 cm⁻¹ line can be assigned to an asymmetric COO⁻ vibration. Its presence in the spectra indicates the formation of a chelate between the side chain –COOH head groups of poly-PCDA and zinc ions from ZnO (see further discussion below). The strength of this interaction (which will depend on the ionic character of the metal oxide) is likely to play a key role in the chromatic reversibility of the red phase in poly-PCDA-metal oxide nanocomposites.⁴³

The 785 nm-laser excited Raman spectra of pure poly-PCDA and of poly-PCDA-ZnO taken at 25 °C in the blue and red phases shown in Fig. 3 were obtained to probe the effect of the interaction between ZnO and side chain head groups on the PDA backbone. Two primary lines at 2086 cm⁻¹ and 1454 cm⁻¹ are observed in the blue phase of poly-PCDA, which can be definitively assigned to the C≡C and C=C stretching modes, respectively, of the polymer backbone. The C=C and the C≡C frequencies at 25 °C downshift relative to the frequencies in the pure polymer by 4 cm⁻¹ in the blue phase of poly-PCDA-ZnO (Fig. 3 and Table 1) which is within the calibrated frequency accuracy of the spectrometer (see, Measurement and techniques). In addition, a line at 2254 cm⁻¹, which is very weak in poly-PCDA increases in intensity in the nanocomposite. The frequency downshifts and increase in intensity of the weak line at 2254 cm⁻¹ are not observed in poly-PCDA nanocomposites with TiO₂ and ZrO₂. In the red phase, the lines due to the C=C and C≡C stretching vibrations in poly-PCDA increase in frequency to 2120 cm⁻¹ and 1514 cm⁻¹, respectively, due to strain on the polymer backbone.⁴⁴ As in the blue phase, the C=C and C≡C stretching vibrations of the red phase of the poly-PCDA-ZnO nanocomposite (Fig. 3 and Table 1) are downshifted relative to the corresponding lines in the red phase of poly-PCDA. A line at 2254 cm⁻¹, probably due to the C≡C

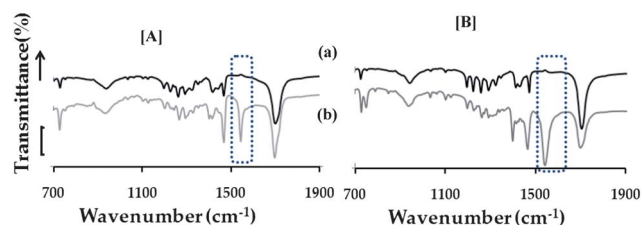


Fig. 2 FTIR spectra at room temperature in the 700–1900 cm⁻¹ range in the blue (panel A) and red (panel B) phases of: (a) pure poly-PCDA, and (b) poly-PCDA-ZnO nanocomposite. The dotted box shows the region around the new line at 1540 cm⁻¹ in the nanocomposite. The height of the square bracket on the left side of the bottom spectrum corresponds to 20% transmittance.

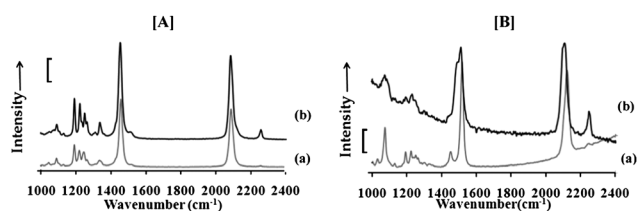


Fig. 3 Raman spectra at 25 °C in the 1000–2400 cm^{-1} frequency range of: A. (a) pure poly-PCDA in the blue phase and (b) poly-PCDA-ZnO in the blue phase, and B. (a) pure poly-PCDA in the red phase and (b) poly-PCDA-ZnO in the red phase. The height of the square bracket on the left side of each panel corresponds to a Raman intensity of 5000 counts/s.

mode of unconverted monomer and/or formation of a diyne,⁴⁵ is observed with increased intensity. Note that the frequencies listed in Table 1 for the red phase were recorded at 175 °C (Fig. 4A). The internal diyne, if present, could form as a defect on the polymer backbone as a result of strain induced on the backbone.⁴⁶

Raman spectra were also obtained on poly-PCDA-ZnO films as a function of temperature by stepwise heating and cooling from room temperature to 200 °C and back to 25 °C using a variable temperature heating stage. Poly-PCDA-ZnO nanocomposite films on silicon wafers were prepared as described in the experimental section. The deposited films in the blue phase were heated at 10 °C min^{-1} and cooled at 5 °C min^{-1} with a holding time of 3 min for recording the Raman spectra. Fig. 4A displays a typical sequence of Raman spectra at different increasing and decreasing temperatures while Fig. 4B shows plots of the C=C and C≡C Raman line frequencies *versus* temperature, which are also listed in Table 2 together with the corresponding temperature and sample color. The C=C and C≡C Raman lines shift to higher frequencies as the temperature was increased from the blue phase at room temperature to an intermediate purple state between 75–100 °C. The C=C and C≡C peak frequencies of the blue phase occur at 1450 cm^{-1} and 2078 cm^{-1} , respectively, and increases to 1482 cm^{-1} and 2102 cm^{-1} in the intermediate purple state. The film changes to the red phase at 175 °C with C=C and C≡C peak frequencies at 1508 cm^{-1} (with a shoulder at 1488 cm^{-1}) and 2106 cm^{-1} , respectively. The weak line near 2250 cm^{-1} discussed above appears with increased intensity both in the red phase and the intermediate purple state. The gradual chromatic changes from blue to purple and then to red occurring on heating suggest increasing strain on the polymer backbone with increasing temperature. On cooling the Raman frequencies and color change back from the red to the blue phase *via* the intermediate purple state (Fig. 4A, right).

Differential scanning calorimetry (DSC) measurements were performed to provide further understanding of the nature of PCDA/poly-PCDA-ZnO interactions. DSC data were obtained for pure PCDA monomer, poly-PCDA, and poly-PCDA-ZnO, at heating and cooling rates of 10 °C min^{-1} between 30 °C and 250 °C. The heating scan for pure PCDA in Fig. 5(a) shows an endothermic peak at 68 °C due to melting. On cooling (scan not shown here) down-shifted exothermic crystallization peaks at 53° and 48 °C due to hysteresis are observed. The heating scan for poly-PCDA in Fig. 5(b) shows an endothermic peak at 68 °C due to melting of the unpolymerized monomer.⁴⁷ A broad endotherm with a shoulder at 184 °C and a peak 197 °C are assigned to the melting of poly-PCDA.⁴⁷ On cooling (scan not shown), polymer crystallization is indicated by broad exothermic features at 245° and 240 °C which are upshifted due to hysteresis relative to the corresponding endothermic melting peaks. Crystallization of unpolymerized monomer is not observed during the cooling cycle probably due to loss of the monomer by sublimation during thermal cycling. The heating scan for poly-PCDA-ZnO [Fig. 5 (c)] shows an endotherm at 68 °C due to unpolymerized monomer and a new endothermic feature at 117 °C due to melting of the monomer modified by chelate formation between the side chain –COOH head groups and Zn ions as noted below. The broad endotherm peaked at 194 °C is likely to be due to melting (with decomposition) of poly-PCDA-ZnO. On cooling, an exotherm due to crystallization of poly-PCDA is observed but there is no evidence for crystallization of the chelate-modified poly-PCDA-ZnO because of decomposition. Also, as observed for poly-PCDA, crystallization of unpolymerized monomer is not detected during the cooling part of the cycle in poly-PCDA-ZnO.

The FTIR, Raman and DSC data discussed above indicate a likely mechanism for reversible thermochromism in poly-PCDA-ZnO based on the interaction of nanoscale ZnO with the head group of the polymer side-chain to form a chelate which can be schematically written as: $\text{Zn}^{2+}(\text{COO}^-)_2$. In pure poly-PCDA, heating causes an irreversible strain on the polymer backbone to form a red phase. In the presence of ZnO, chelate formation would result in release of strain on cooling and reversal back to the blue phase.

Effect of ZnO crystallite size on thermochromism in poly-PCDA-ZnO

An interesting feature is the fact that PDA-ZnO composite formation with reversible thermochromism occurs only when nanocrystalline ZnO is used. Thermochromic changes were investigated in poly-PCDA-ZnO composites prepared using ZnO

Table 1 C=C and C≡C Raman peak frequencies in pure poly-PCDA and in poly-PCDA-ZnO nanocomposite in the blue and red phases

Phase	Poly-PCDA, 25 °C		Poly-PCDA-ZnO [Blue, 25 °C; Red 175 °C ^a]	
	$\nu(\text{C}=\text{C}) \text{ cm}^{-1}$	$\nu(\text{C}\equiv\text{C}) \text{ cm}^{-1}$	$\nu(\text{C}=\text{C}) \text{ cm}^{-1}$	$\nu(\text{C}\equiv\text{C}) \text{ cm}^{-1}$
Blue	1454	2086	1450	2082, 2254 ^c
Red	1514, 1442 (sh) ^b	2120	1506, 1488(sh)	2102, 2248 ^c

^a Data from Fig. 4A. ^b sh – shoulder. ^c See text for interpretation of these lines.

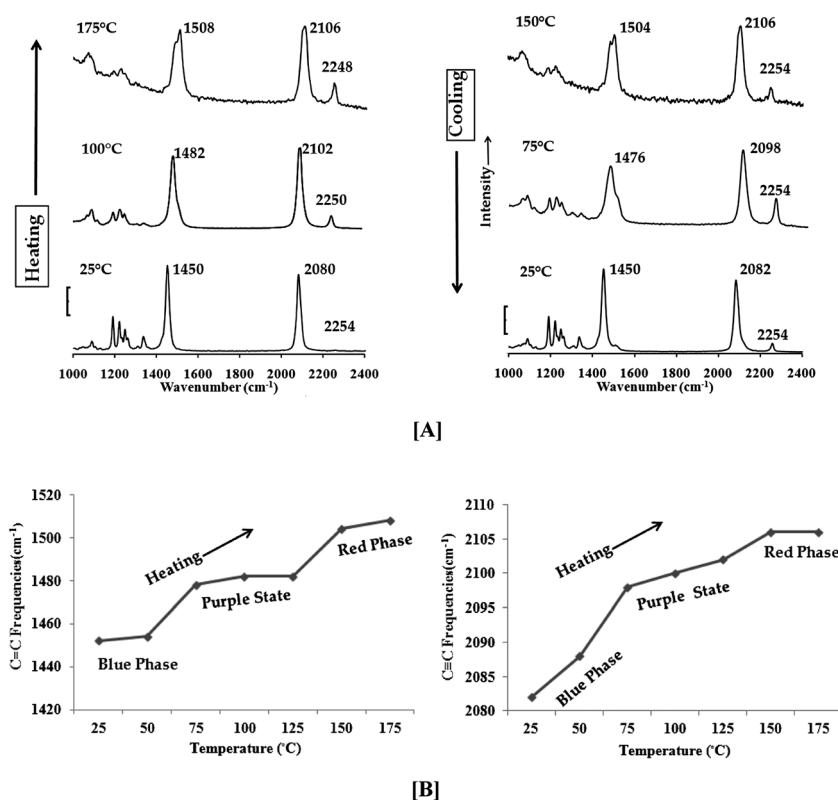


Fig. 4 [A] Raman spectra of a poly-PCDA-ZnO nanocomposite film as a function of temperature during heating (left panel) and cooling (right panel). The heights of the square brackets on the left hand side of the bottom spectra correspond to a Raman intensity of 10 000 counts/s, and [B] $\nu(\text{C}=\text{C})$ and $\nu(\text{C}\equiv\text{C})$ Raman frequencies as a function of temperature during heating of the poly-PCDA-ZnO nanocomposite film. The approximate temperature ranges of the three chromatic phases are indicated in the figures.

Table 2 Raman frequencies assigned to different chromatic states in poly-PCDA-ZnO as a function of increasing and decreasing temperature

Temperatures, °C	$\nu(\text{C}=\text{C})$ frequencies, cm^{-1}	$\nu(\text{C}\equiv\text{C})$ frequencies, cm^{-1}	Film Color
25	1450	2078	Blue
75	1482	2096	Blue/Purple
100	1482	2102	Pink/Purple
175	1508	2106	Red
150	1506	2100	Red
125	1506	2100	Pink
105	1482	2104	Pink/Purple
95	1478	2098	Blue
25	1450	2078	Blue

with four different average crystallite or particle sizes determined by laser diffraction measurements.

Particle sizes of ZnO used ranged from 2.1 to 11000 nm (Table 3) to give poly-PCDA-ZnO composites. Composites with reversible thermochromism using ZnO in the crystallite size range from 300 nm and below were used, suggesting that the head group-ZnO interaction discussed above is impeded when the crystallite size of ZnO is above 300 nm. Raman spectra of ZnO of different crystallite sizes were therefore recorded to analyze the structural differences among the ZnO samples. The Raman spectra of 2.1 and 300 nm size ZnO are compared with the spectra of 1000 and 11000 nm ZnO in Fig. 6. The primary

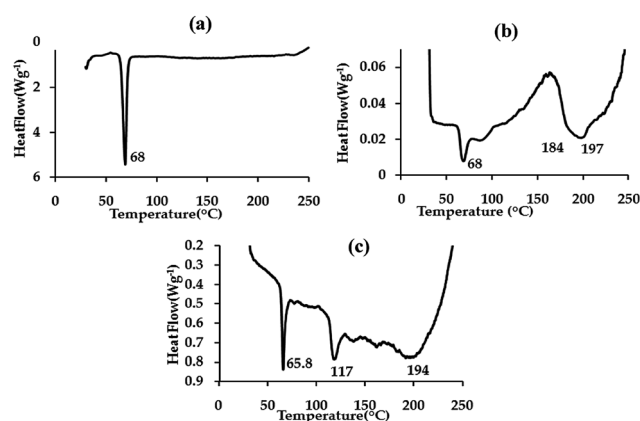
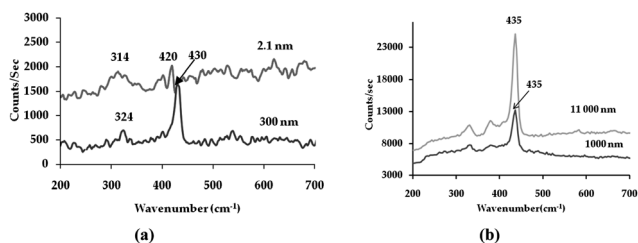


Fig. 5 Differential scanning calorimetry (DSC) heating scans at a heating rate of 10°C per minute for: (a) the PCDA monomer, (b) poly-PCDA, and (c) poly-PCDA-ZnO.

Raman line at 435 cm^{-1} narrows somewhat and becomes intense in the spectrum for 11000 nm size ZnO relative to the spectrum of 1000 nm ZnO (Fig. 6b). In the nanosized 2.1 and 300 nm samples (Fig. 6a), the 435 cm^{-1} broadens toward lower frequencies and shifts down in frequency to 420 and 430 cm^{-1} , respectively, most likely due to well known phonon localization effects.⁴⁸ Moreover, there is substantial broadening of the line at 314 cm^{-1} in 2.1 nm ZnO indicating increased grain boundary amorphous

Table 3 Thermochromism of poly-PCDA-ZnO composites using different crystallite sizes of ZnO as determined by light diffraction

ZnO	Average crystalline size (nm)	Thermochromic transition
nanocrystalline	2.1	Rapidly reversible
nanocrystalline	300	Reversible
Crystalline (Sigma-Aldrich, Puriss)	1000	Irreversible
Nanocrystalline ZnO (300 nm) annealed at 1100 °C	11 000	Irreversible

**Fig. 6** Raman spectra between 200 and 700 cm^{-1} of: (a) nanocrystalline 2.1 nm and 300 nm size ZnO; and (b) 1000 nm size ZnO from Aldrich and 11000 nm size annealed ZnO.

fraction in nanosized ZnO⁴⁹ where interaction with the polymer side chain head group would likely occur.

UV-visible spectra recorded at 25 °C of poly-PCDA-ZnO prepared using 1000, 11000, and 300 nm ZnO are shown in Fig. 7. The spectra are the same as that of poly-PCDA in the blue and red phases. In the blue phase an excitonic peak at ~ 640 nm with a vibronic component at ~ 590 nm⁵⁰ is observed. In the red phase the excitonic peak is blue-shifted due to decreased conjugation length to ~ 540 nm and the vibronic peak is downshifted to ~ 490 nm. No size induced absorption energy changes were observed.

XANES and EXAFS (Fig. 8) measurements were also conducted to probe the electron density and atomic structure, respectively, around the metal atom in the poly-PCDA-ZnO composites contrasting the 2.1 nm and 300 nm ZnO and the poly-PCDA-ZnO composites. The XANES data in Fig. 8 (a) show marked size effects on the position of the main 1s–4p peak that shifts to the higher energies for 300 nm particles compared to the 2.1 nm ones. This effect is in full agreement with theoretical calculations of Kuzmin *et al.*⁵¹ The EXAFS data obtained for the larger sizes are in good agreement with previous measurements on poly-PCDA-ZnO prepared using 300 nm ZnO and published elsewhere.⁴⁶ The spectrum shown in Fig. 8 (b) indicates decreased

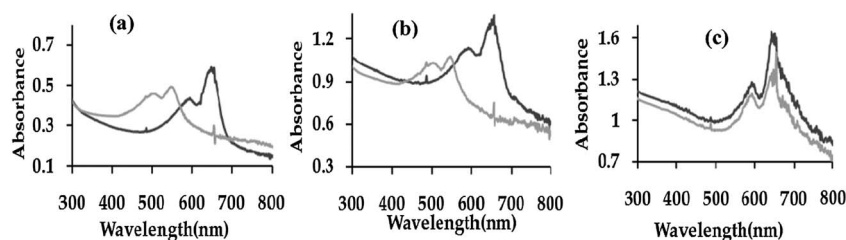
disorder in the Zn–O and Zn–Zn shells in the composite relative to that in the pure ZnO sample of 2.1 nm in size.

Due to the substantial grain boundary amorphous content indicated by the Raman data for this sample, only a weak peak in the region of the Zn–Zn shell is observed. These effects are in contrast to very little change observed in both the Zn–O shell and the Zn–Zn shell in poly-PCDA-ZnO (compared to its pure ZnO counterpart) prepared using 300 nm ZnO. The latter observation is consistent with the large size of the particles. Further work is under way to understand the origin of enhanced ordering in the local environment around Zn in poly-PCDA-ZnO prepared using 2.1 nm ZnO.

Thermochromism in poly-PCDA-Zr_{1-x}Zn_xO_y composites

In an effort to decrease the rate of the reversible thermochromic transition in poly-PCDA-ZnO composites for elapsed time-temperature sensing applications, poly-PCDA composites were prepared using heat-treated mixed oxides of ZnO and ZrO₂. The Raman spectra of annealed ZnO compared with that of annealed ZrO₂ and ZnO/ZrO₂ alloys of nominal composition Zr_{1-x}Zn_xO_y, with $x = 0.2$ and 0.5 , are shown in Fig. 9A. The spectra indicate that the primary line in ZnO at 435 cm^{-1} shows substantial weakening as a result of alloy formation. The XRPD patterns of poly-PCDA, ZnO/ZrO₂ and of poly-PCDA-Zr_{1-x}Zn_xO_y $x = 0.2$ displayed in Fig. 9B show shifts to smaller angles due to lattice expansion on composite formation. In addition, two closely spaced new reflections appear around 33 degrees in the composite. Further work would be needed to determine the crystallographic changes that occur with composite formation.

In order to determine whether the chromatic transition from the red phase back to the blue phase is effected, for example, slowed down from a few minutes in poly-PCDA-ZnO to hours or days in poly-PCDA-Zr_{1-x}Zn_xO_y $x = 0.2$, chromaticity (corresponding to the saturation level of a particular hue of a color) measurements were carried out using an X-rite optical

**Fig. 7** UV-visible spectra at 25 °C of poly-PCDA-ZnO composites with three different crystallite sizes of ZnO: (a) poly-PCDA with ZnO (1000 nm) in irreversible red (gray) and blue (black) phases, (b) poly-PCDA with annealed ZnO (11000 nm) in irreversible red (gray) and blue (black) phases, and (c) poly-PCDA with nanocrystalline ZnO (300 nm) showing the spectrum in the reversible red phase which rapidly converts back to blue (gray) and the spectrum in the blue phase (black).

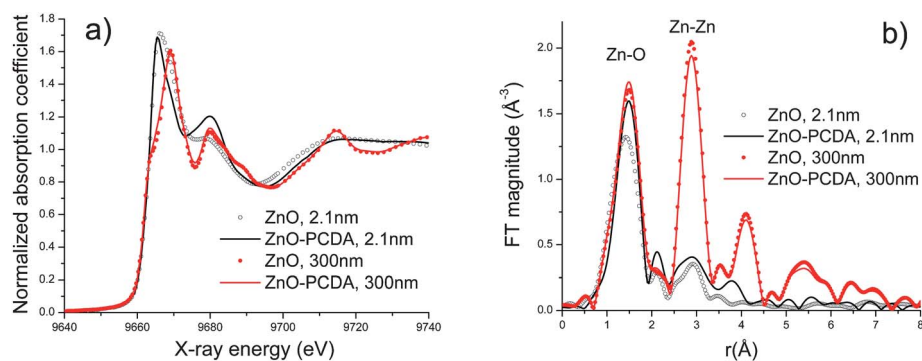


Fig. 8 XANES (a) and Fourier transform magnitudes of k^2 -weighted EXAFS (b) spectra for different ZnO particle sizes, 2.1 and 300 nm. Both energy and r -space plots show that the poly-PCDA-ZnO complex has a more ordered structure than its ZnO counterpart for the 2.1 nm size. Both systems have very weak Zn-Zn coordination compared to that for pure ZnO and poly-PCDA-ZnO complex of 300 nm in size. The 300 nm size particles show weaker PCDA complexation effects (due to their larger size) than the 2.1 nm particles.

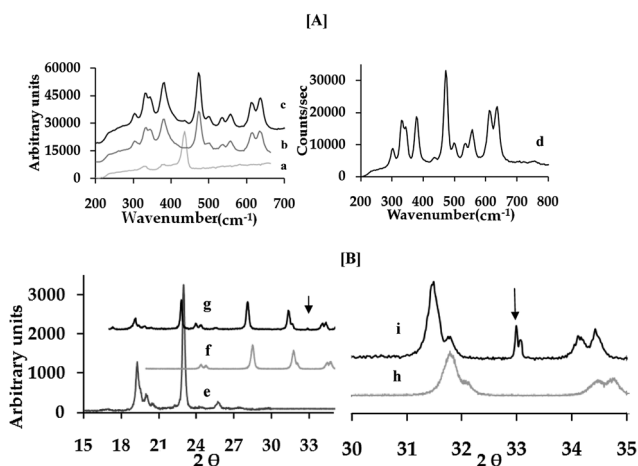


Fig. 9 A. Raman spectra of: (a) annealed ZnO, b) annealed ZrO_2 , c) heat-treated ZnO/ ZrO_2 mixture of composition $Zr_{1-x}Zn_xO_y$, $x = 0.2$ and d) heat-treated ZnO/ ZrO_2 mixture of composition $Zr_{1-x}Zn_xO_y$, $x = 0.5$ corresponding to equal amounts of ZnO and ZrO_2 . B. XRPD patterns of: e) poly-PCDA, f) ZnO/ ZrO_2 of composition $Zr_{1-x}Zn_xO_y$, $x = 0.2$, g) poly-PCDA- $Zr_{1-x}Zn_xO_y$, $x = 0.2$, and h) and i) expanded XRPD patterns between 30 and 35 degrees of $Zr_{1-x}Zn_xO_y$, $x = 0.2$ and poly-PCDA- $Zr_{1-x}Zn_xO_y$, $x = 0.2$. Arrows indicate the position of the new lines that appear in the diffraction pattern of poly-PCDA- $Zr_{1-x}Zn_xO_y$, $x = 0.2$.

densitometer. These measurements were made at 25 °C for a poly-PCDA- $Zr_{1-x}Zn_xO_y$ $x = 0.2$ sample thermally transformed to the red phase. The data shown in Fig. 10 indicate that the chromaticity of the red phase in poly-PCDA- $Zr_{1-x}Zn_xO_y$ $x = 0.2$ is indeed slowed down, decreasing slowly over days from the red back to the blue phase. By contrast the chromaticity of poly-PCDA-ZnO changes back to the blue phase in a few minutes. Composites of the poly-PCDA with the mixed oxides can therefore be used for elapsed time-temperature sensing applications.

Conclusions

Raman, FTIR, DSC, uv-visible and XAFS data have been used to understand the thermochromic reversibility introduced by

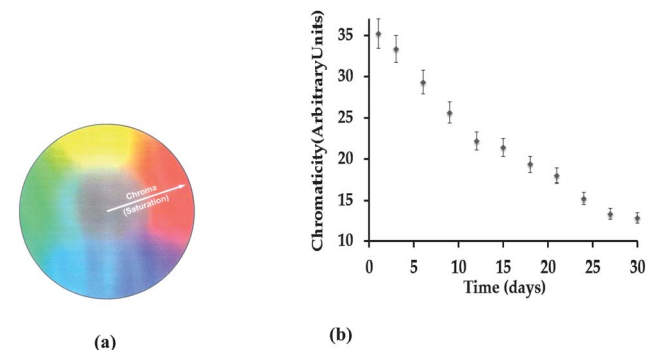


Fig. 10 (a) Schematic showing chromaticity (chroma) distributions from gray or dull at the center to vivid or saturated at the perimeter; and (b) plot of chromaticity values measured using an optical densitometer as a function of time in days at 25 °C for a poly-PCDA-ZnO/ ZrO_2 composite thermally transformed to the red phase and then cooled to 25 °C.

composite formation of poly-PCDA with nanocrystalline ZnO in the size range below 300 nm. Poly-PCDA composites with nanocrystalline TiO_2 and ZrO_2 in the same size range however do not affect the irreversibility of the thermochromic transition. It was proposed that chelate formation between ZnO and side chain head group $-COOH$ leads to reversibility of the thermochromic transition. Raman and XRPD data together with optical chromaticity data are presented to show that ZnO alloyed with ZrO_2 form poly-PCDA-mixed oxide composites with slowed down reversibility to the blue phase, thus allowing the use of these composites for elapsed time-temperature sensors.

Acknowledgements

AP and ZI were supported by the US Army, ARDEC contract W15QKN-10-D-0503-0002. A.I.F. acknowledges support by the U.S. Department of Energy Grant DE-FG02-03ER15476. Beamlines X18B and X19A at the NSLS are supported in part by the Synchrotron Catalysis Consortium, U.S. Department of Energy Grant No DE-FG02-05ER15688. The authors thank Professors D.S. Lee and K.W. Lem, Konkuk National University, Seoul, South Korea, for providing a sample of nano-sized

zinc oxide. The authors would also like to thank one of the reviewers for insightful comments which have helped to substantially improve the paper.

References

- R. W. Carpick, D. Y. Sasaki, M. S. Marcus, M. A. Eriksson and A. R. Burns, *J. Phys.: Condens. Matter*, 2004, **16**, R679–R697.
- U. Jonas, K. Shah, S. Norvez and D. H. Charych, *J. Am. Chem. Soc.*, 1999, **121**, 4580–4588.
- S. Wu, L. Niu, J. Shen, Q. Zhang and C. Bubeck, *Macromolecules*, 2009, **42**, 362–367.
- D. S. Johnston, S. Sanghera, M. Pons and D. Chapman, *Biochim. Biophys. Acta*, 1980, **602**, 57–69.
- A. Singh and J. M. Schnur, *Polym. Prepr.*, 1985, **26**, 184–185.
- B. Hupfer, H. Ringsdorf and H. Schupp, *Chem. Phys. Lipids*, 1983, **33**, 355–374.
- S. Y. Okada, R. Jelinek and D. Charych, *Angew. Chem., Int. Ed.*, 1999, **38**, 655–659.
- D. H. Charych, Q. Cheng, A. Reichert, G. Kuziemko, M. Stroh, J. O. Nagy, W. Spevak and R. C. Stevens, *Chem. Biol.*, 1996, **3**, 113–120.
- Q. Cheng and R. C. Stevens, *Adv. Mater.*, 1997, **9**, 481–483.
- A. Berman, D. J. Ahn, A. Lio, M. Salmeron, A. Reichert and D. Charych, *Science*, 1995, **269**, 515–518.
- S. Kolusheva, T. Shahal and R. Jelinek, *J. Am. Chem. Soc.*, 2000, **122**, 776–780.
- J. J. Pan and D. Charych, *Langmuir*, 1997, **13**, 1365–1367.
- Q. Huo, K. C. Russell and R. M. Leblanc, *Langmuir*, 1999, **15**, 3972–3980.
- Z. Ma, J. Li, M. Liu, J. Cao, Z. Zhou, J. Tu and L. Jiang, *J. Am. Chem. Soc.*, 1998, **120**, 12678–12679.
- S. Kolusheva, R. Kafri, M. Katz and R. Jelinek, *J. Am. Chem. Soc.*, 2001, **123**, 417–422.
- R. Jelinek, *Drug Dev. Res.*, 2000, **50**, 497–501.
- T. Kim, K. C. Chan and R. M. Crooks, *J. Am. Chem. Soc.*, 1997, **119**, 189–193.
- R. H. Baughman, *J. Appl. Phys.*, 1972, **43**, 4362–4370.
- K. C. Lim and A. J. Heeger, *J. Chem. Phys.*, 1985, **82**, 522–530.
- R. R. Chance, R. H. Baughman, H. Muller and C. J. Eckhardt, *J. Chem. Phys.*, 1977, **67**, 3616–3618.
- Y. Tokura, T. Kanetake, K. Ishikawa and T. Koda, *Synth. Met.*, 1987, **18**, 407–412.
- W. Yuan, G. Jiang, Y. Song and L. Jiang, *J. Appl. Polym. Sci.*, 2007, **103**, 942–946.
- P. T. Hammond and M. F. Rubner, *Macromolecules*, 1997, **30**, 5773–5782.
- X. Huang, S. Jiang and M. Liu, *J. Phys. Chem. B*, 2005, **109**, 114–119.
- H. Peng, J. Tang, J. Pang, D. Chen, L. Yang, H. S. Ashbaugh, C. J. Brinker, Z. Yang and Y. Lu, *J. Am. Chem. Soc.*, 2005, **127**, 12782–12783.
- H. Peng, J. Tang, L. Yang, J. Pang, H. S. Ashbaugh, C. J. Brinker, Z. Yang and Y. Lu, *J. Am. Chem. Soc.*, 2006, **128**, 5304–5305.
- J. Song, J. S. Cisar and C. R. Bertozzi, *J. Am. Chem. Soc.*, 2004, **126**, 8459–8465.
- L. S. Li and S. I. Stupp, *Macromolecules*, 1997, **30**, 5313–5320.
- Y. Yang, Y. Lu, M. Lu, J. Huang, R. Haddad, G. Xomeritakis, N. Liu, A. P. Malanoski, D. Sturmayer, H. Fan, D. Y. Sasaki, R. A. Assink, J. A. Shelnett, F. V. Swol, G. P. Lopez, A. R. Burns and C. J. Brinker, *J. Am. Chem. Soc.*, 2003, **125**, 1269–1277.
- D. J. Ahn, E. H. Chae, G. S. Lee, H. Y. Shim, T. E. Chang, K.-D. Ahn and J. M. Kim, *J. Am. Chem. Soc.*, 2003, **125**, 8976–8977.
- J. M. Kim, J. S. Lee, H. Choi, D. Sohn and D. J. Ahn, *Macromolecules*, 2005, **38**, 9366–9376.
- S. Lee and J. M. Kim, *Macromolecules*, 2007, **40**, 9201–9204.
- H. Park, J. S. Lee, H. Choi, D. J. Ahn and J.-M. Kim, *Adv. Funct. Mater.*, 2007, **17**, 3447–3455.
- Z. Yuan, C.-W. Lee and S.-H. Lee, *Angew. Chem., Int. Ed.*, 2004, **43**, 4197–4200.
- Y. Gu, W. Cao, L. Zhu, D. Chen and M. Jiang, *Macromolecules*, 2008, **41**, 2299–2303.
- A. Singh, R. B. Thompson and J. M. Schnur, *J. Am. Chem. Soc.*, 1986, **108**, 2785–2787.
- J. Pang, L. Yang, B. F. McCaughey, H. Peng, H. S. Ashbaugh, C. J. Brinker and Y. Lu, *J. Phys. Chem. B*, 2006, **110**, 7221–7225.
- S. Balakrishnan, S. Lee and J.-M. Kim, *J. Mater. Chem.*, 2010, **20**, 2302–2304.
- T. Itoh, T. Shichi, T. Yui, H. Takahashi, Y. Inui and K. Takagi, *J. Phys. Chem. B*, 2005, **109**, 3199–3206.
- Y. Wang, Ph.D. Thesis, University of Massachusetts, Lowell, MA, 2007.
- Y. Wang, L. Li, K. Yang, L. A. Samuelson and J. Kumar, *J. Am. Chem. Soc.*, 2007, **129**, 7238–7239.
- Y. Wang, K. Yang, S.-C. Kim, R. Nagarajan, L. A. Samuelson and J. Kumar, *Chem. Mater.*, 2006, **18**, 4215–4217.
- Z.-H. Tang and B.-A. Yang, *J. Mater. Sci.*, 2007, **42**, 10133–10137.
- M. Wenzel and G. H. Atkinson, *J. Am. Chem. Soc.*, 1989, **111**, 6123–6127.
- C. Lim, D. J. Sandman and M. Sukwattanasinitt, *Macromolecules*, 2008, **41**, 675–681.
- A. Patlolla, Q. Wang, A. Frenkel, J. L. III. Zunino, D. R. Skelton and Z. Iqbal, *MRS Online Proc. Libr.*, 2009, **1190**, NN11–04.
- N. Mino, H. Tamura and K. Ogawa, *Langmuir*, 1991, **7**, 2336–2341.
- V. S. Gorelik, S. N. Miko, M. I. Sokolovskii and T. Tsuzuki, *Inorg. Mater.*, 2006, **42**, 282–285.
- S. Siddique, R. K. Chhaya, P. Arun and N. C. Mehra, *Phys. Lett. A*, 2008, **372**, 7068–7072.
- J. A. Diaz-Ponce, O. G. Morales-Saavedra, M. F. Beristain-Manterola, J. M. Hernandez Alcantara and T. Ogawa, *J. Lumin.*, 2008, **128**, 1431–1441.
- A. Kuzmin, S. Larcheri and F. Rocca, *J. Phys. Conf. Ser.*, 2007, **93**, 012045.